Development 133, 3983-3992 (2006) doi:10.1242/dev.02583

Semaphorin 3d promotes cell proliferation and neural crest cell development downstream of TCF in the zebrafish hindbrain

Jason D. Berndt and Mary C. Halloran*

Neural crest cells (NCCs) are pluripotent migratory cells that are crucial to the development of the peripheral nervous system, pigment cells and craniofacial cartilage and bone. NCCs are specified within the dorsal ectoderm and undergo an epithelial to mesenchymal transition (EMT) in order to migrate to target destinations where they differentiate. Here we report a role for a member of the semaphorin family of cell guidance molecules in NCC development. Morpholino-mediated knockdown of Sema3d inhibits the proliferation of hindbrain neuroepithelial cells. In addition, Sema3d knockdown reduces markers of migratory NCCs and disrupts NCC-derived tissues. Similarly, expression of a dominant-repressor form of TCF (ΔTCF) reduces hindbrain cell proliferation and leads to a disruption of migratory NCC markers. Moreover, expression of ΔTCF downregulates *sema3d* RNA expression. Finally, Sema3d overexpression rescues reduced proliferation caused by ΔTCF expression, suggesting that Sema3d lies downstream of Wnt/TCF signaling in the molecular pathway thought to control cell cycle in NCC precursors.

KEY WORDS: Neural crest, Zebrafish, Semaphorin, TCF, Cell cycle, Cyclin

INTRODUCTION

Neural crest cells (NCCs) are a population of pluripotent precursor cells that arise from the border of the neural ectoderm during neurulation and migrate through the extracellular space to multiple targets in the embryo. There they differentiate into several cell types, including neurons, glia, pigment cells, cartilage and bone (Le Douarin and Kalcheim, 1999). To begin migration, NCCs delaminate from the neuroepithelium, which requires an EMT. During EMT, cells downregulate epithelial cell adhesions in favor of adhesion to the extracellular matrix and undergo changes in cell morphology that allow them to migrate (Duband et al., 1995; Hay, 1995). NCCs undergo cell division before and throughout their migration and differentiation (Kalcheim and Burstyn-Cohen, 2005). Precise regulation of the proliferation of NCCs and their precursors is probably crucial for their development. Wnt signaling plays a role in controlling the G1- to S-phase transition of trunk NCCs, and this is thought to be required for the onset of NCC migration (Burstyn-Cohen et al., 2004). However, little is known about what other factors may control NCC proliferation or the role of the cell cycle in subsequent NCC development.

We have investigated the role of a semaphorin, Sema3d, in hindbrain NCC development in the zebrafish. Semaphorins constitute a large family of signaling molecules originally identified as axon guidance cues (Kolodkin, 1998). Semaphorins also guide migrating cells (Tamagnone and Comoglio, 2004). Class 3 semaphorins are secreted and bind to heteromeric receptors containing members of the plexin and neuropilin protein families (Yu and Kolodkin, 1999). Signaling through these receptors is thought to regulate the cytoskeleton of axonal growth cones and migratory cells, in part, through the activity of Rho GTPases (Tamagnone and Comoglio, 2000; Liu and Strittmatter, 2001; Pasterkamp and Kolodkin, 2003; Negishi et al., 2005).

Departments of Zoology and Anatomy and Neuroscience Training Program, University of Wisconsin, Madison, WI 53706, USA.

*Author for correspondence (e-mail: mchalloran@wisc.edu)

Accepted 11 August 2006

Semaphorins have been implicated previously in the control of NCC migration. Sema3a inhibits the migration of chick NCCs in vitro and is expressed in regions bordering NCC migration pathways in vivo (Eickholt et al., 1999). Disruption of Sema3a or Sema3f signaling in vivo causes NCCs to invade normally NCC-free zones, suggesting that these semaphorins act to inhibit NCCs from straying outside their pathway (Osborne et al., 2005). Similarly, class 3 semaphorins are proposed to maintain appropriate separation of hindbrain migratory NCC streams in zebrafish (Yu and Moens, 2005). In other contexts, semaphorins may also attract NCCs. In mice, Sema3c is expressed in the cardiac outflow tract, a target to which NCCs fail to migrate in Sema3c knockout mice (Brown et al., 2001; Feiner et al., 2001). Semaphorin receptors are also implicated in NCC migration. When neuropilin 1 expression is inhibited in chick, NCCs destined to form sympathetic neurons are unable to complete their migration (Bron et al., 2004). A similar phenotype is seen in neuropilin 1-null mice (Kawasaki et al., 2002). Thus, semaphorins and their receptors play an important role in the migration of NCCs across species. Here, we show a different role for a semaphorin in controlling proliferation of NCC precursors.

In zebrafish, Sema3d and neuropilins are expressed in subsets of cranial NCCs prior to the onset of migration (Halloran et al., 1999; Yu et al., 2004), suggesting a potential role in NCC development. We show that Sema3d loss of function leads to a decrease in the number of migratory NCCs and a disruption in the development of NCC derivatives. Furthermore, we unexpectedly found that Sema3d knockdown leads to reduced proliferation of hindbrain neuroepithelial cells at the time of NCC production. Cell proliferation in NCC precursors has been linked to Wnt signaling (Burstyn-Cohen et al., 2004). We also show that the inhibition of Wnt/TCF signaling via expression of ΔTCF leads to the inhibition of hindbrain cell proliferation and migratory NCC markers. Moreover, *sema3d* expression is eliminated by expression of ΔTCF. Finally, overexpression of Sema3d partially rescues the reduced cell proliferation, suggesting that Sema3d lies downstream of Wnt/TCF signaling in this pathway.

MATERIALS AND METHODS

Embryos

Wild-type (AB) zebrafish (*Danio rerio*) embryos were obtained from natural matings. For Sema3d overexpression studies, Tg(*hsp70:sema3d*^{myc}) (Liu et al., 2004) embryos were obtained from homozygote incrosses. For TCF inhibition studies, Tg(*hsp70*:ΔTCF^{gfp}) (Lewis et al., 2004) embryos were obtained from hemizygous outcrosses to *leopard* strain. Double transgenic embryos were obtained from Tg(*hsp70:sema3d*^{myc}) homozygote crosses to Tg(*hsp70*:ΔTCF^{gfp}) hemizygotes and screened by GFP fluoresence. Embryos were reared at 25-29.5°C in E3 embryo medium and staged according to Kimmel et al. (Kimmel et al., 1995). Hours or days post fertilization (hpf and dpf) were defined as time reared at 28.5°C. Heat-induction of transgenes was performed by transferring embryos in 100 ml E3 in glass beakers from 28.5°C to 39.5°C for 1 hour. Embryos were then returned to 28.5°C for recovery until BrdU treatment and/or fixation.

Morpholino design and injection

Morpholino oligonucleotides were synthesized by Gene Tools (Corvalis, OR). Lyophilized morpholinos were resuspended in sterile water at a concentration of 2 mM. Morpholinos were further diluted in 1× Danieau solution (Nasevicius and Ekker, 2000) with 0.1% Phenol Red to the working concentration. Optimal doses, defined as the highest dose that did not significantly increase mortality or cause overt non-specific necrosis, were determined empirically. Approximately 1 nl was injected into the yolks of embryos at the one- to four-cell stage. In some cases, morpholinos conjugated to FITC were used. This tag did not affect the efficacy of the morpholino (not shown).

Sema3d translation inhibition morpholino (3DMO, 5′-catgatggacgaggagatttctgca-3′) and four-base mismatch control morpholino (5′-cat*c*atg*c*acgaggaga*a*atct*c*ca-3′) were used at 100 or 250 μM (Liu et al., 2004; Wolman et al., 2004). Additionally, either of two Sema3d splice blocking morpholinos was injected at 500 μM. These were designed to complement the boundaries of the fourth intron/fifth exon (3DI4E5MO, 5′-cacattcagtctgcagcaagagaaa-3′) and fourth exon/fourth intron (3DE4I4MO, 5′-ctgactgatacttacaagagggttt-3′). In some experiments, we also used a random sequence control morpholino (5′-cctcttacctcagttacaatttata-3′) at 500 μM. Sema3d splice morpholinos were tested by RT-PCR on total RNA isolated from embryos with Trizol (Invitrogen) using the following primers: RT, 5′-tgg aac tgg tag tgg tga ac-3′; forward, 5′-cca gac aac atc aat aaa cac ccc-3′; reverse, 5′-ttg ccc agg aaa tca gac gc-3′. Sequencing of individual, gel-purified bands was performed by the UW-Biotechnology Center (Madison, WI). Sequence analysis was conducted using MacVector (Accelrys, San Diego, CA).

In situ hybridization

In situ hybridization was performed at 67°C with digoxigenin or FITC-labeled riboprobes as in Halloran et al. (Halloran et al., 1999). Digoxigenin or FITC was localized immunohistochemically with an antibody conjugated to alkaline phosphatase (Roche, Indianapolis, IN) and with NBT/BCIP as a substrate.

crestin and *dlx2* double-labeling experiments were performed according to Jowett (Jowett, 1999). Quantification was performed by outlining the rhombomere 4 migratory stream in images collected by epifluoresence and automated calculation of the integrated area by Metamorph (Universal Imaging, Dowington, PA).

Phosphohistone-H3 and BrdU labeling

Phosphorylated histone H3 was recognized by a rabbit polyclonal antibody (Upstate Bio, NY) and detected with the Vector ABC kit (Vector Labs, CA) or Alexa 568 secondary antibodies. PH3-positive nuclei were counted by eye on a Nikon TE3000 inverted microscope at 600× magnification. Nuclei were counted in rhombomeres 3, 4 and 5 throughout the entire dorsal ventral extent of the neuroepithelium.

S-phase nuclei were identified by 5-bromo-2-deoxyuridine (BrdU) incorporation as described (Shepard et al., 2004). Immunohistochemistry for BrdU (mouse anti-BrdU, Roche, Indianapolis, IN) was performed using Alexa 488- or Alexa 568-conjugated secondary antibodies (Molecular Probes, Eugene, OR). Embryos were flat-mounted dorsal side towards the coverslip in an anti-fade solution (Hjorth and Key, 2001). Images were collected every 1 μm to a depth of 40 μm from the dorsal surface with a BioRad MRC 1024 laser-scanning confocal microscope. Experimental and control embryos were always imaged during the same session using the same settings on the microscope and software. Nuclei were counted in rhombomeres 3, 4 and 5 on one side of the neural tube in a single optical plane at the level of the dorsal otocyst.

Alcian blue

Cartilage was labeled with 0.1% (w/v) Alcian Blue (Sigma) essentially as described (Schilling et al., 1996), except that the dilution buffer consisted of 0.37% HCl and 70% ethanol, and trypsinization was not performed. Lower jaws were dissected and flat-mounted.

FITC-uncaging

One cell stage embryos were injected with 2% DMNB-caged FITC-dextran (10×10^3 M_r, Molecular Probes, Eugene, OR). At 15 hpf, embryos were dechorionated, arrayed in depression wells, and bathed in E3. The fluorophore was uncaged via illumination at 360 nm with a 60× dipping objective. Exposure for 1 second through a pinhole aperture was controlled by an automated shutter. Embryos were fixed 2 hours later, counter-stained with 0.2% TOPRO3 (Molecular Probes, Eugene, OR), and flat mounted for confocal imaging. The number of uncaged cells adjacent to the neuroepithelium was quantified.

RESULTS

sema3d is expressed in hindbrain NCCs

In zebrafish, cranial NCCs initially arise lateral to the neuroepithelium in two anteroposterior bands from the midbrain through the hindbrain (Schilling and Kimmel, 1994). Subsequently, NCCs also arise from the neuroepithelium proper (J.D.B. and M.C.H., unpublished). NCCs begin migration around 14-15 hpf and segregate into three distinct streams lateral to rhombomeres 2, 4 and 6. We have reported previously that *sema3d* is expressed in rhombomeres 3, 4 and 5, and in migratory NCCs (Halloran et al., 1999). A more detailed analysis of *sema3d* expression confirms this initial expression pattern and reveals additional expression in other premigratory NCCs. As early as 11-12 hpf, *sema3d* expression is initiated in the hindbrain and premigratory NCCs (not shown). By 15 hpf, *sema3d* is expressed strongly in rhombomeres 3, 4 and 5 and in rhombomere 2 (Fig. 1A). Transverse sections through rhomobomere 4 at this stage reveal that expression is restricted to the dorsal neuroepithelium (Fig. 1B). Expression is also apparent in premigratory and early migratory NCCs adjacent to rhombomere 4 (Fig. 1A,B). Despite this initial restriction, *sema3d* is eventually expressed in all three migratory streams, i.e. adjacent to rhombomeres 2, 4 and 6 (Halloran et al., 1999). Ultimately, *sema3d* is expressed in the mandibular, hyoid and gill pharyngeal arches (Halloran et al., 1999) (Fig. 1C). Thus, *sema3d* is expressed in a dynamic pattern during premigratory and migratory NCC stages, suggesting that it may play a role in NCC development.

Sema3d knockdown causes abnormalities in a subset of NCC derivatives

In order to investigate the role of Sema3d in NCC development, we examined the effects of Sema3d knockdown on NCC derivatives in the head. We injected newly fertilized embryos with a Sema3d translation blocking morpholino (3DMO) (Liu et al., 2004; Wolman et al., 2004), or one of two control morpholinos (CONMO): a random sequence control morpholino or one containing four mispaired bases relative to 3DMO. To control for potential non-specific effects of the morpholino, we also used two Sema3d splice-blocking morpholinos (3DI4E5MO and 3DE4I4MO). RT-PCR and sequencing of Sema3d cDNA from morpholino injected embryos showed that 3DI4E5MO caused an 118 nucleotide in-frame deletion

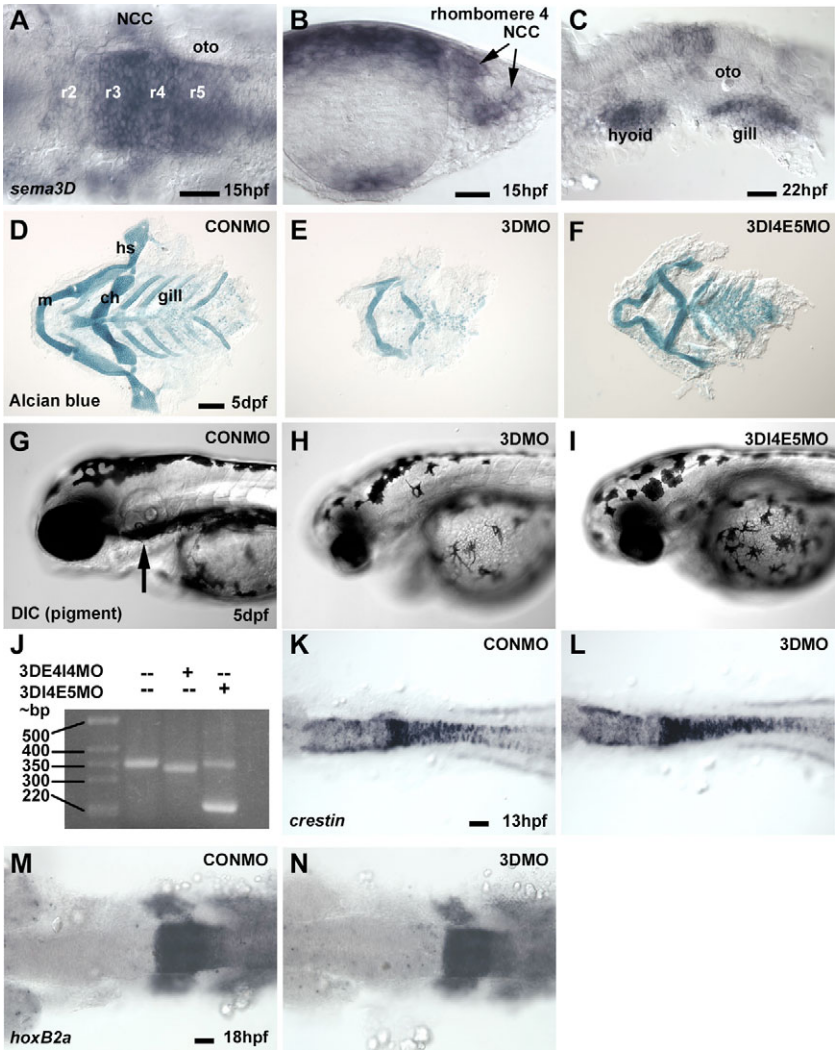

Fig. 1. Sema3d mRNA is expressed in NCCs and morpholino knockdown of Sema3d disrupts NCC derivatives without affecting NCC induction. (**A-C**) In situ hybridization for *sema3d* at 15 hpf (A,B) and 22 hpf (C). (**D-F**) Alcian Blue labeling of pharyngeal cartilage at 5 dpf; (**G-I**) DIC imaging of melanophores in 2 dpf in CONMO (D,G), 3DMO (E,H) and 3DI4E5MO (F,I) injected embryos. Arrow in G indicates ventral horn of melanophores. (**J**) RT-PCR on mRNA extracted from embryos injected with Sema3d splice blocking morpholinos. (**K-N**) In situ hybridization for *crestin* at 13 hpf (K,L) and *hoxb2a* at 18 hpf (M,N) in CONMO (K,M) and 3DMO (L,N) injected embryos. (A,K-N) Dorsal views, anterior is leftwards. (B) Transverse section through rhombomere 4. (C,G-I) Lateral views, anterior is leftwards. (D-F) Ventral views, anterior is leftwards. r2-r5, rhombomeres 2-5; oto, otocyst; m, hs, ch and gill, Meckel's, hyosymplectic, ceratohyal and gill cartilages, respectively; bp, base pairs. Scale bars: 40 μm for A,C,M,N; 20 μm for B; 100 μm for D-I; 80 μm for K,L.

corresponding to nucleotides 656-775 of Sema3d (GenBank Accession Number, NM_131048, Fig. 1J). This deletion removed a region of the Sema domain, including a predicted N-glycosylation site. 3DE4I4MO caused a small variable deletion (15-20 nucleotides within the Sema domain) (Fig. 1J, deletion begins at nucleotide 656 and has a variable 3′ end). Embryos in this and subsequent experiments were stage-matched to correct for delay caused by morpholino injection.

NCCs give rise to cranial cartilage, peripheral nervous system components, and pigment cells. Thus, we analyzed these cell types following Sema3d knockdown. Embryos injected with 3DMO showed dramatic reductions and malformations of lower jaw cartilage when compared with CONMO-injected embryos (Fig. 1D,E). This phenotype varied from the complete absence of cartilage (not shown) to milder reductions in the size of the Meckel's and ceratohyal cartilages accompanied by a loss of the hyosymplectic and gill cartilages (Fig. 1E). 3DI4E5MO or 3DE4I4MO-injected embryos displayed a similar range and quality of phenotype as 3DMO-injected embryos (Fig. 1F; data not shown), suggesting that Sema3d knockdown specifically disrupts patterning of the jaw. We also examined non-ectomesenchymal NCC derivatives. We observed pigment cells in living embryos from 2 to 5 dpf. 3DMO and 3DI4E5MO-injected embryos had reduced numbers of melanophores relative to CONMO-injected and uninjected embryos (Fig. 1G-I and not shown). This reduction was most severe in the ventral horn of melanophores in the head (arrow in Fig. 1G). Immunohistochemistry for the HuC/D antigen at 48 hpf labels the neurons of peripheral cranial ganglia. We did not detect a difference in HuC/D immunoreactivity between CONMO and 3DMO-injected embryos (not shown). Moreover, we did not detect differences in the glia of these ganglia between CONMO and 3DMO-injected embryos, as detected by *foxd3* expression at 36 hpf (not shown). Collectively, these results suggest that Sema3d expression in the NCCs and hindbrain is necessary for the development of some but not all cranial NCC-derivatives.

Sema3d knockdown does not alter NCC induction or hindbrain patterning

To understand the function of Sema3d and determine the stage of NCC development at which it is required, we analyzed each step of NCC development. To test whether defects in NCC derivatives were due to a failure of initial NCC induction, we analyzed markers of premigratory NCCs. Prior to the onset of migration, NCCs are found in two bands lateral to the neuroepithelium. In addition, NCCs arise from a region overlying and within the neuroepithelium. We found no difference in the expression of two premigratory NCC markers, *crestin* (Rubinstein et al., 2000; Luo et al., 2001) and *snail1b* (previously *snail2*) (Thisse et al., 1995), in these regions between 3DMO and CONMO-injected embryos at 13 hpf (Fig. 1K,L and not shown). We also examined premigratory NCC markers at later

stages of development. At 17 hpf we saw no reduction in *foxd3* (Odenthal and Nusslein-Volhard, 1998; Kelsh et al., 2000), *sox9a/sox9b* (Chiang et al., 2001), *sox10* (Dutton et al., 2001) or *snail1b* expression (not shown). Because NCCs are formed from dorsal ectoderm, the absence of changes in the expression of premigratory NCC markers suggests that Sema3d knockdown does not alter dorsoventral patterning in the hindbrain. In addition, we examined the anteroposterior patterning of the hindbrain because different numbers of NCCs are generated from different rhombomeres (Lumsden et al., 1991). Thus, anteroposterior fate transformations could conceivably alter the number of migratory NCCs and NCC derivatives. We labeled 3DMO and CONMO-injected embryos at 17 hpf for *hoxb1a*, *hoxb2a*, *hoxb3a* or *hoxa2b* (Prince et al., 1998), or for *krox20* (Oxtoby and Jowett, 1993), each of which is expressed with specific anteroposterior boundaries. We did not detect differences in the placement, size or compartmentalization of rhombomeres between 3DMO and CONMO-injected embryos (Fig. 1M,N; not shown). Collectively, these data show that the defects in NCC derivatives caused by Sema3d knockdown are not due to large scale changes in NCC induction or hindbrain patterning.

Sema3d does not affect the NCC EMT

Following their induction, NCCs undergo an EMT to begin migration; inhibition of EMT could lead to defects in NCC derivatives. In order to test whether Sema3d is required for EMT, we counted the number of NCCs that underwent the EMT during a 2-hour time period in Sema3d knockdown embryos. We co-injected embryos with either 3DMO or CONMO and caged-FITC dextran at the one-cell stage. To label a subset of NCC precursors in the neuroepithelium, we photo-uncaged the fluorophore in a small region of rhombomeres 4 and 6 at 15 hpf. Embryos were fixed 2 hours later, counterstained with TOPRO3 to label all nuclei, and imaged on a confocal microscope (Fig. 2A,B). We found no difference in the number of FITC-labeled migratory NCCs adjacent to rhombomeres 4 or 6 between CONMO and 3DMO-injected embryos (Table 1) (rhombomere 4, P=0.20; rhombomere 6, P=0.39; t-test). These data suggest that the EMT of NCCs from the hindbrain neuroepithelium at 15-17 hpf is not dependent on Sema3d.

Sema3d knockdown causes a reduction in migratory NCC markers

The next stage in NCC development is migration from the neural tube. We used markers of migratory NCCs to test whether Sema3d knockdown alters the number of migrating NCCs or disrupts the pattern of NCC migration. At 18 hpf, we labeled embryos by in situ hybridization for *crestin* and *dlx2* (Akimenko et al., 1994). Wild-type and CONMO-injected embryos expressed *crestin* normally in the three migratory streams of hindbrain NCCs (Fig. 2C; not shown). By contrast, 3DMO-injected embryos showed a strong reduction in *crestin* labeling (Fig. 2D). 3DE4I4MO and 3DI4E5MO-injected embryos also showed reduced *crestin* expression in hindbrain NCCs (Fig. 2E; not shown). We counted the number of embryos showing reduced *crestin* labeling. We found that 13% and 17% of uninjected and CONMO-injected embryos, respectively, showed a reduction; whereas, 72%, 68% and 56% of 3DMO, 3DI4E5MO and 3DE4I4MO-injected embryos, respectively, showed a reduction. The reductions in Sema3d knockdown embryos were statistically significant compared to controls ($P<10^{-7}$ for all comparisons, z-test, n=272 uninjected, n=214 CONMO, n=118 3DMO, n=122 3DI4E5MO, n=55 3DE4I4MO). *Dlx2* is expressed in NCCs migrating to the pharyngeal arches. Following Sema3d knockdown

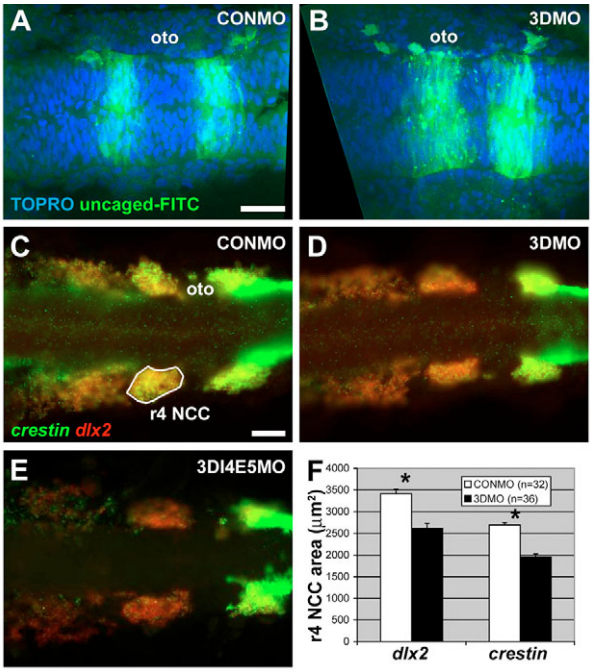

Fig. 2. Sema3d knockdown reduces migratory NCC markers without affecting EMT. (**A**,**B**) Uncaged FITC-dextran (green) and TOPRO3 labeling of nuclei (blue) in the hindbrain at 17 hpf in CONMO (A) and 3DMO (B) injected embryos. (**C-E**) Double in situ hybridization for *crestin* (green) and *dlx2* (red); expression is reduced in 3DMO (D) and 3DI4E5MO (E) injected embryos compared with CONMO (C). (**F**) Quantification of the area of labeling of *crestin* and *dlx2* in the r4 migratory stream, indicated by white outline in C. *$P<10^{-6}$, t-test. (A-E) Dorsal views, anterior is leftwards. oto, otocyst. Scale bars: 40 μm.

by 3DMO or 3DI4E5MO, *dlx2* expression was also reduced, although not as severely as *crestin* (Fig. 2C-E). To quantify the reduction, we used double-fluorescent in situ hybridization to label *crestin* and *dlx2* in the same embryos. In whole mounts and sections of wild-type embryos, we found that the expression regions of *dlx2* and *crestin* largely overlap (not shown). We measured the area of labeling of both genes in the rhombomere 4 migratory stream. We found a significant reduction in the area of labeling with both genes in 3DMO-injected embryos relative to CONMO-injected (Fig. 2F). The area of *crestin* expression was reduced by 27%, and the area of *dlx2* expression was reduced by 23%. This suggests that 3DMO-injected embryos have fewer migratory NCCs or that NCCs are less dispersed compared with CONMO-injected embryos. Nevertheless, the intensity of *crestin* labeling was more drastically reduced than that of *dlx2*, suggesting that Sema3d knockdown may affect the expression of *crestin* in addition to affecting the migration of NCCs.

Sema3d knockdown reduces cell proliferation in the hindbrain

Because the gross pattern of NCC migration was intact in Sema3d knockdown embryos, we explored an alternative mechanism for the defects in migratory NCCs and NCC derivatives described above. NCCs undergo extensive proliferation before and after migration. Furthermore, progression from the G1 to S phase of the cell cycle is required for the onset of migration in chicken trunk NCCs (Burstyn-Cohen and Kalcheim, 2002; Burstyn-Cohen et al., 2004). Although semaphorins have not been implicated in cell cycle regulation, we

Table 1. Number of migratory NCCs 2 hours after uncaging FITC-dextran

Mean±s.e.m.	Rhombomere 4	Rhombomere 6
CONMO (*n*=42)	3.0±0.44	3.1±0.34
3DMO (*n*=41)	3.7±0.37	3.6±0.42

analyzed the effect of Sema3d knockdown on the numbers of neuroepithelial cells in G2/M phase or S phase by immunolabeling for PH3 and incorporated BrdU, respectively. We found a reduction in the number of proliferating hindbrain neuroepithelial cells at 17 hpf in 3DMO-injected embryos compared with CONMO-injected embryos (Fig. 3A-D). The number of BrdU-positive nuclei in the dorsal neuroepithelial regions that strongly expresses *sema3d*, i.e. rhombomeres 3, 4 and 5, was significantly reduced in 3DMO (27% reduction, $P<10^{-8}$) and 3DI4E5MO-injected embryos (18% reduction, $P<10^{-7}$) when compared with CONMO (Fig. 3E). Likewise, the number of PH3-positive nuclei in the same region was also significantly reduced in 3DMO (29% reduction, $P<10^{-7}$) and 3DI4E5MO-injected embryos (24% reduction, $P<10^{-4}$) compared with CONMO-injected embryos (Fig. 3F). Thus, Sema3d knockdown leads to a reduction in the proliferation of NCC precursors.

In order to address the temporal and spatial specificity of the reduction in cell proliferation, we analyzed PH3 expression at other times and in other tissues of 3DMO and CONMO-injected embryos. As described above, we found that PH3 labeling was reduced in the hindbrain at 18 hpf (Table 2). By contrast, at a time before the onset of Sema3d expression (10 hpf), the number of PH3 labeled nuclei in the future neuroepithelium was unaffected by 3DMO injection (Table 2). Similarly, when we counted PH3 labeled nuclei in the hindbrain at later times of development (24 and 36 hpf), we did not find a difference between 3DMO and CONMO-injected embryos (Table 2). Furthermore, PH3 labeling in other regions of the embryo where Sema3d is not expressed, e.g. the eye, was not affected. Interestingly, in two regions that express Sema3d, the spinal cord and pharyngeal arches, Sema3d knockdown increased the number of PH3-positive nuclei (Table 2). Collectively, these data suggest that Sema3d regulates cell proliferation in a specific spatiotemporal pattern and that hindbrain neuroepithelial cell proliferation is selectively reduced during the time of NCC production.

Sema3d knockdown affects cyclin gene expression

The cell cycle duration in neuroepithelial cells during the early stages of *sema3d* expression (~12 hpf) is about 4-5 hours (Kimmel et al., 1994). As the inhibition of Sema3d protein by morpholino injection is constitutive, the analysis of PH3 and BrdU at 17 hpf in Sema3d knockdown embryos reflects the cumulative effects of more than one round of cell cycle. To discern which phase of the cell cycle is affected, we examined the expression of several cyclins and cyclin-dependent kinase inhibitor proteins (KIPs). Cyclin D1 transcript and protein levels increase during the G1 phase of the cell cycle. In the above studies, a low concentration (100 μM) of 3DMO was sufficient to decrease cell proliferation (Fig. 3) (Table 2). At this dose, we did not detect differences in *cyclin D1* transcript levels. However, when we injected the same morpholino at a higher concentration (250 μM), the expression of *cyclin D1* was increased in 3DMO-injected embryos relative to CONMO (Fig. 4A,B). Similarly, 3DI4E5MO injection increased *cyclin D1* expression relative to CONMO-injected and uninjected embryos (Fig. 4C). We next examined two cyclins expressed in the G2 phase of the cell cycle, *cyclin A2* and *cyclin B1*. Both *cyclin A2* and *cyclin B1* were decreased in 3DMO and 3DI4E5MO-injected embryos relative to controls (Fig. 4D-F; not shown). Cyclin E2 mRNA, another G1 cyclin, was not affected by Sema3d knockdown (not shown). Finally, we examined the expression of two *kinase inhibitor proteins*, *p27kip1* (*cdkn1b* – Zebrafish Information Network) and *p57kip2* (*cdkn1c* – Zebrafish Information Network), which are expressed in G1 and direct cells toward cell cycle exit (G0). Notably, both *p27kip1* and *p57kip2* were increased in rhombomere 4 in 3DMO-injected embryos relative to CONMO-injected embryos (Fig. 4G-I; not shown). Collectively, these data suggest that Sema3d knockdown causes G1/G0 cell cycle arrest.

Sema3d knockdown increases cell death specifically in the dorsal hindbrain

Cell cycle arrest can lead to cell death. Reduced proliferation and/or increased cell death of NCCs or NCC precursors could explain the disruption of NCC development after Sema3d knockdown. At a low concentration of the morpholino (100 μM) (at which we saw defects in proliferation, migratory NCCs and derivatives), we did not find overt necrosis or apoptosis in 3DMO-injected embryos using direct

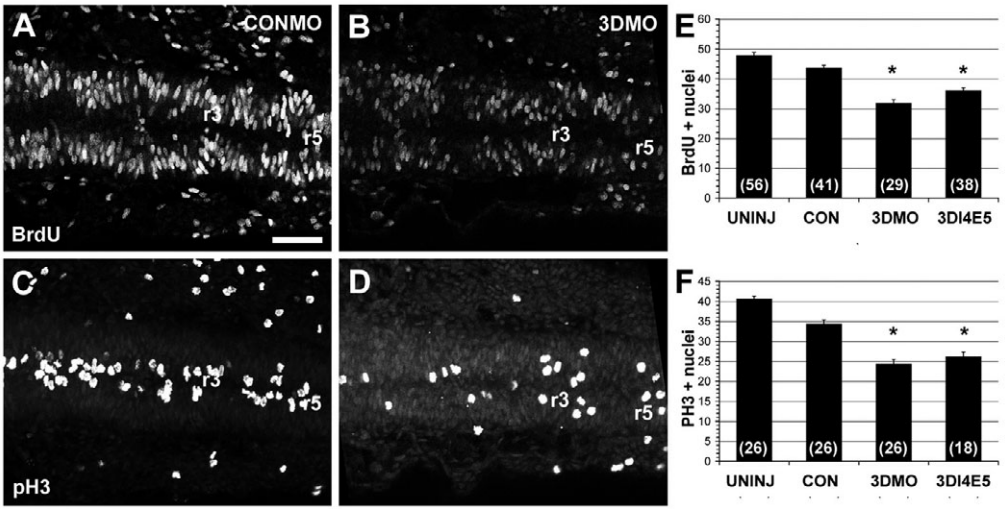

Fig. 3. Sema3d knockdown inhibits cell cycle in the hindbrain.
(**A-D**) Immunodetection in the hindbrain at 17 hpf of BrdU (A,B) and PH3 (C,D) in CONMO (A,C) and 3DMO (B,D) injected embryos. (**E**,**F**) Quantification of the number of BrdU (E) and PH3 (F) labeled nuclei in the neuroepithelium of rhombomeres 3-5. Numbers in parentheses indicate *n*. **P*<10^{-4} compared with CONMO, *t*-test. (A-D) Dorsal views, anterior is leftwards. Scale bar: 40 μm for A-D.

Table 2. Phosphohistone-H3 positive nuclei

Mean±s.e.m.		10 hpf	18 hpf	24 hpf	36 hpf
Cranial neuroepithelium	CONMO	26±1.6	27±1.0	30±2.1	28±1.7
	3DMO	29±0.9	22±1.3*	28±3.5	30±2.2
Spinal neuroepithelium	CONMO	ND	14±0.4	16±0.6	14±1.3
	3DMO	ND	17±0.9†	17±1.0	14±1.0
Eye	CONMO	ND	26±2.3	46±1.4	31±1.6
	3DMO	ND	30±2.8	44±3.0	32±3.4
Otocyst	CONMO	ND	5±0.6	8±0.5	10±0.8
	3DMO	ND	6±0.5	8±0.8	10±0.8
Tailbud	CONMO	ND	14±1.1	7±0.5	6±1.1
	3DMO	ND	12±0.7	7±1.0	5±0.7
Pharyngeal arches	CONMO	ND	ND	24±2.3	12±0.8
	3DMO	ND	ND	23±1.9	14±0.9*

*P<0.005, †P<0.02.

observation or by labeling with Acridine Orange or TUNEL at 17 or 22 hpf (not shown). At a high concentration (250 μM) (at which we saw changes in expression of cyclin genes), we saw some necrosis and apoptosis in the brain that appeared to gradually increase between 12-24 hpf, the period when Sema3d is expressed (not shown). We analyzed cell death at 24 hpf and found that the number of Acridine Orange-labeled cells was increased in 3DMO-injected or 3DI4E5MO-injected relative to CONMO-injected embryos (see Fig. S1A,B in the supplementary material). These changes were limited to the dorsal hindbrain and NCC-forming regions (see Fig. S1C-H in the supplementary material). We did not detect an increase in the ventral hindbrain neuroepithelium, the eye or the spinal cord. Together, these data suggest a specific pattern of cell death related to Sema3d function rather than non-specific morpholino-related toxicity.

Sema3d overexpression rescues aspects of Sema3d knockdown

We investigated whether Sema3d overexpression could rescue the NCC and proliferation defects caused by Sema3d knockdown. We overexpressed Sema3d using a stable transgenic line containing *myc*-tagged *sema3d* (Sema3d^{myc}) controlled by the *hsp70* promoter (Liu et al., 2004; Sakai and Halloran, 2006). First, we asked whether Sema3d overexpression affected *cyclin D1* expression. We overexpressed Sema3d^{myc} by heat-shocking Sema3d^{myc} transgenic embryos for 1 hour at 14 hpf and analyzed *cyclin D1* transcript levels at 17 hpf. We found that heat-shock induced overexpression of Sema3d^{myc} decreased *cyclin D1* expression relative to non-heat-shocked Sema3d^{myc} transgenic and heat-shock wild-type controls (see Fig. S2A,B in the supplementary material and not shown). Furthermore, Sema3d^{myc} overexpression restored normal *cyclin D1* levels in 3DI4E5MO-injected transgenic embryos (see Fig. S2C,D in the supplementary material), whereas heat-shock alone in wild-type embryos did not (see Fig. S2E,F in the supplementary material).

Next, we asked whether Sema3d overexpression affected PH3 and/or BrdU labeling. We heat-shocked wild-type and Sema3d^{myc} transgenic embryos for 1 hour at 14 hpf and assayed for PH3 and BrdU labeling at 17 hpf. Neither heat-shock induced Sema3d overexpression in Sema3d^{myc} transgenic embryos nor heat-shock alone in wild-type embryos affected the number of PH3-positive nuclei (see Fig. S2H in the supplementary material). By contrast, Sema3d^{myc} overexpression significantly reduced BrdU incorporation (see Fig. S2G in the supplementary material). Surprisingly, heat shock alone in wild-type embryos also reduced BrdU labeling (see Fig. S2G in the supplementary material). However, Sema3d^{myc} transgenic embryos were not as severely affected by heat-shock as were wild-type embryos (heat-shock Sema3d^{myc} versus heat-shock wild type, P<0.03) (see Fig. S2G in the supplementary material). Thus, Sema3d^{myc} overexpression counteracted the effects of heat-shock alone. This suggests that

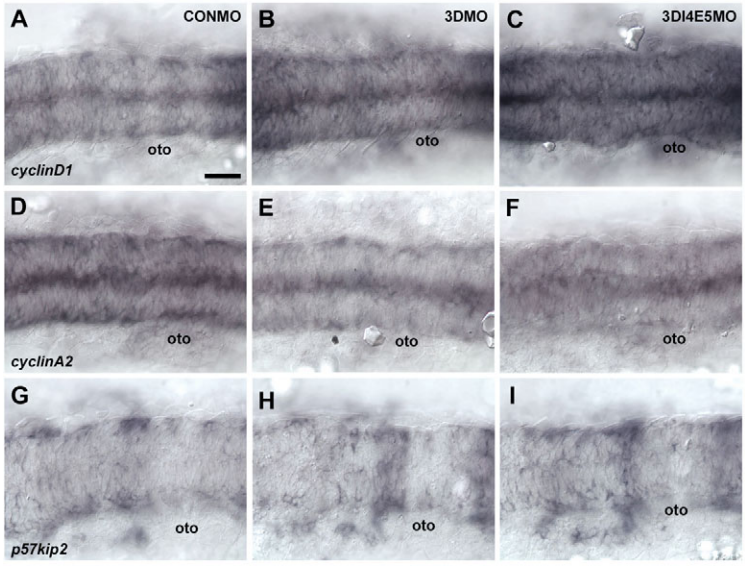

Fig. 4. Sema3d knockdown affects the expression of cell cycle genes. (**A-I**) In situ hybridization in the hindbrain at 17hpf for *cyclin D1* (A-C), *cyclin A2* (D-F) and *p57kip2* (G-I) in CONMO (A,D,G), 3DMO (B,E,H), and 3DI4E5MO (C,F,I) injected embryos. oto, otocyst. (A-I) Dorsal views, anterior is leftwards. Scale bars: 40 μm for A-I.

Sema3d overexpression promotes the transition to S phase. As morpholino-mediated knockdown of Sema3d led to a loss of both PH3 and BrdU, we asked whether Sema3d^{myc} overexpression could rescue these effects. Unexpectedly, Sema3d^{myc} overexpression failed to rescue the decreases in PH3 or BrdU caused by 3DI4E5MO-mediated Sema3d knockdown (see Fig. S2G,H in the supplementary material).

Finally, we asked whether Sema3d overexpression could rescue defects in *crestin* expression or NCC derivatives. We overexpressed Sema3d^{myc} by heat-shocking transgenic embryos for 1 hour at 14 hpf and analyzed *crestin* at 18 hpf. Sema3d^{myc} overexpression alone did not change *crestin* expression and failed to rescue the reduction in *crestin* following Sema3d knockdown by 3DI4E5MO (not shown). Moreover, Sema3d^{myc} overexpression induced by heat-shock for 1 hour at 14 hpf or for 1 hour at 14, 24, 36, 48, 60, 72 and 84 hpf, did not cause aberrant cartilage or pigment phenotypes at 5 dpf and did not rescue the cartilage or pigment phenotypes produced by 3DI4E5MO injection (not shown).

Sema3d overexpression rescues decreased proliferation caused by TCF inhibition

Because cell cycle was disrupted by Sema3d knockdown, we examined the possibility that Sema3d is in the molecular pathway thought to control cell cycle in NCCs. Canonical Wnt signaling, which activates TCF-dependent transcription, is crucial for the G1/S transition in NCCs (Burstyn-Cohen et al., 2004) as in other systems (Tetsu and McCormick, 1999). Therefore, we asked whether this is also true for hindbrain NCCs in zebrafish embryos. We employed a transgenic line containing a dominant-repressor form of TCF (ΔTCF^{gfp}) driven by the *hsp70* promoter (Lewis et al., 2004). Using this line, Lewis et al. (Lewis et al., 2004) found that the induction of ΔTCF^{gfp} before the six-somite stage (12 hpf) leads to a failure of NCC specification. Therefore, we activated the transgene after this period. Induction of ΔTCF^{gfp} by heat shock for 1 hour at 14 hpf resulted in a significant reduction in the number of BrdU-labeled nuclei at 17 hpf (Fig. 5A,B,J, 43% reduction, $P<10^{-13}$, *t*-test). As expected, ΔTCF^{gfp} expression also reduced *crestin* expression (Fig. 5C,D) and eliminated *cyclin D1* (Fig. 5E,F). Notably, expression of ΔTCF^{gfp} resulted in the elimination of *sema3d* expression (Fig. 5G,H). Analysis of the genomic sequence revealed at least three potential TCF-binding sites in the 5′ sequence proximal to the *sema3d*-coding region (not shown), suggesting the potential for direct transcriptional regulation by TCF. Thus, we tested whether Sema3d^{myc} overexpression could rescue the ΔTCF^{gfp} phenotype. We crossed Sema3d^{myc} to ΔTCF^{gfp} fish to produce double transgenic embryos. We heat induced expression of both transgenes and analyzed BrdU incorporation and *crestin* expression. Sema3d^{myc} overexpression significantly increased the number of BrdU-labeled nuclei in ΔTCF^{gfp}-expressing embryos (Fig. 5I,J, 40% increase, $P<10^{-4}$, *t*-test). *crestin* expression was not restored by overexpression of Sema3d^{myc} in ΔTCF^{gfp} expressing embryos (not shown). These data suggest that Sema3d acts downstream of TCF and upstream of the cell cycle but in parallel with other Wnt/TCF downstream factors necessary for NCC development.

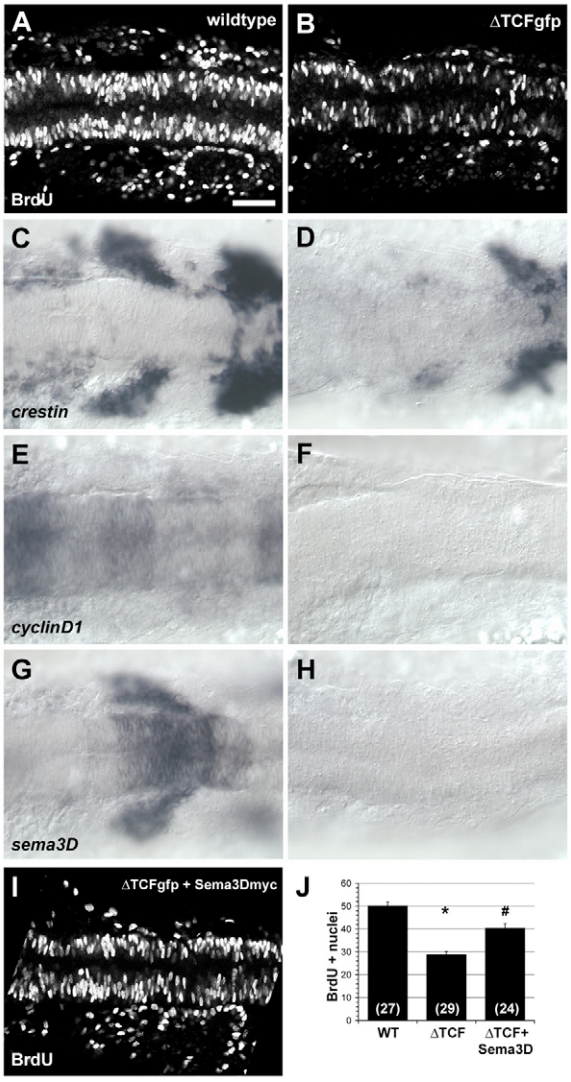

Fig. 5. ΔTCF^{gfp} disrupts cell cycle and *crestin* expression and eliminates *cyclin D1* and *sema3d* expression.
(**A-I**) Immunodetection of BrdU (A,B,I) and in situ hybridization for *crestin* (C,D), *cyclinD1* (E,F), *sema3d* (G,H) in the hindbrain at 17 hpf of heat-shocked wild-type siblings (A,C,E,G), ΔTCF^{gfp} transgenic (B,D,F,H), and ΔTCF^{gfp} + Sema3d^{myc} double-transgenic (I) embryos.
(**J**) Quantification of the number of BrdU-labeled nuclei in the neuroepithelium of rhombomeres 3-5. Numbers in parentheses indicate *n*. *$P<10^{-13}$ versus wild-type sibling, #$P<10^{-4}$ versus ΔTCF^{gfp}, *t*-test.
(A-I) Dorsal views, anterior is leftwards. oto, otocyst. Scale bar: 40 μm for A-I.

DISCUSSION

These experiments provide evidence for a novel role for a semaphorin in the regulation of cell cycle and NCC development. Sema3d is expressed in a dynamic pattern in the dorsal hindbrain and migratory NCCs. Neuropilins also are expressed in the hindbrain and migratory NCCs (Yu et al., 2004). Although Sema3d is a secreted protein, there is evidence that class 3 semaphorins associate with the extracellular matrix and neuropilins on the surface of cells secreting them (De Wit et al., 2005). Thus, Sema3d could act via autocrine or paracrine signaling on NCCs or their precursors. We found that knockdown of Sema3d caused a reduction in migratory NCC markers and defects in a subset of NCC derivatives (Figs 1, 2). These effects occurred in the absence of effects on premigratory NCCs or patterning of the hindbrain neuroepithelium (Fig. 1). Sema3d knockdown also inhibited cell proliferation in the hindbrain (Fig. 3). A reduction in proliferation of NCC precursors alone could cause reduced numbers of migratory cells and subsequent defects in NCC derivatives. In addition, because cell cycle has been linked to the NCC EMT, it is also possible that

Sema3d could affect the EMT. However, our results suggest that Sema3d knockdown does not negatively regulate the NCC EMT. In our photo-uncaging experiments, we examined the number of NCCs undergoing the EMT during a period less than the length of one cell cycle. This allowed us to minimize the contribution of differences in cell number caused by cell proliferation changes and to emphasize potential differences in cell motility. Thus, we were able to test the EMT largely independently of changes in cell cycle. Because we did not exhaustively test all times during NCC production or all regions of the hindbrain, we cannot rule out the possibility that Sema3d regulates the EMT. However, taken together our results are consistent with a mechanism in which the primary role of Sema3d is to regulate the cell cycle of NCCs with the potential to affect the NCC EMT.

Interestingly, a separate class of ligands, vascular endothelial growth factors (VEGFs), can bind to the semaphorin receptor neuropilin, and are known to regulate cell proliferation and migration in tissues with invasive migratory behavior similar to NCCs, e.g. endothelial cells and carcinomas (Ferrara et al., 2003; Tammela et al., 2005). There is evidence that VEGFs compete with class 3 semaphorins for neuropilin binding (Miao et al., 1999; Bagnard et al., 2001). Furthermore, zebrafish $VEGF_{165}$ is expressed by NCCs (Yu et al., 2004), which suggests that this competition may be relevant to NCC proliferation and EMT.

Previous work has shown that Wnt/TCF signaling controls cell cycle in NCCs as well as the induction and EMT of NCCs (Chang and Hemmati-Brivanlou, 1998; LaBonne and Bronner-Fraser, 1998; Burstyn-Cohen et al., 2004; Lewis et al., 2004). We show that *sema3d* expression can be regulated by TCF and that $Sema3d^{myc}$ overexpression can rescue cell cycle inhibition caused by the inhibition of Wnt/TCF (Fig. 5). The simplest model for these data is a linear relationship whereby Sema3d is an effector of the Wnt/TCF pathway (Fig. 6A). However, although $Sema3d^{myc}$ rescued the reduced BrdU incorporation caused by ΔTCF, it did not rescue the reduction caused by Sema3d knockdown (see Fig. S2A in the supplementary material). Moreover, TCF inhibition leads to decreases in *cyclin D1*, while Sema3d knockdown leads to increases in *cyclin D1* (Figs 4, 5). These findings argue against a direct linear relationship. Thus, we propose an alternative model that could explain our data (Fig. 6B). According to this model, Wnt/TCF and Sema3d interact in a more complex feedback loop. Wnt/TCF is the primary regulator of the molecular machinery controlling the G1/S transition, Sema3d has the capacity to modulate this pathway, and Wnt/TCF can feedback onto Sema3d. We propose that this feedback is both positive, through the activation of *sema3d* transcription, and negative, through the activation of an unknown inhibitor of Sema3d. Thus, TCF repression would inhibit both Sema3d and the unknown inhibitor. In this scenario, we expect Sema3d to play a modulatory role on the timing of the cell cycle, and its activity and/or expression could be required in a specific temporal or spatial pattern, perhaps regulated by Wnt/TCF. This model suggests several predictions that are supported by our data. First, the expression of the dominant repressor, ΔTCF, would downregulate Sema3d. Second, Sema3d overexpression would rescue ΔTCF because of the downregulation of the inhibitor. Finally, when ΔTCF is not expressed, Sema3d overexpression would not rescue Sema3d knockdown because of the presence of the inhibitor.

This complex relationship suggests that Sema3d may have the capacity to regulate the Wnt/TCF pathway. Recent evidence suggests that semaphorins can directly regulate the Wnt pathway. Sema4d was found to activate GSK3β, a component of the Wnt/TCF pathway, and the activation of GSK3β was required for

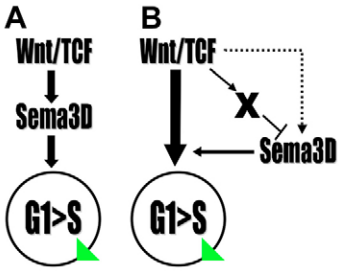

Fig. 6. Schematic models of potential interactions between Wnt/TCF and Sema3d. (**A**) A linear model with Sema3d signaling downstream of Wnt/TCF. (**B**) An alternative model showing the interaction of parallel pathways by means of an unidentified inhibitor, X.

Sema4d-mediated growth cone collapse (Ito et al., 2006). The two pathways also share the ability to affect both the cell cycle and cell adhesions, and thus there are multiple points where the pathways might converge. For example, integrins are known to be important for NCC EMT and migration (Perris and Perissinotto, 2000). Two semaphorins, Sema3a and Sema4d, have been shown to modulate integrin signaling (Serini et al., 2003; Barberis et al., 2004; Toyofuku et al., 2005). Furthermore, integrin-linked kinase is able to regulate Cyclin D1 protein and mRNA through GSK3β in cancers and mammary epithelial cells (D'Amico et al., 2000; Tan et al., 2001). Cells in culture require attachment to the substratum in order to progress from G1 to S phase of the cell cycle (Aplin et al., 1999; Danen and Yamada, 2001). Thus, loss of attachment of NCCs to the extracellular matrix and the resulting loss of integrin activation could result in aberrant cell cycle. Interestingly, we found that membrane blebbing, which can be regulated by attachment to the extracellular matrix (Sugrue and Hay, 1981), is increased following Sema3d knockdown (J.D.B. and M.C.H., unpublished).

Exciting recent studies show that the cell cycle and cell migration are intimately connected. In addition to its role in cell cycle control, p27(KIP1) inhibits the activation of the small GTPase RhoA in cultured mammalian cells (Besson et al., 2004). The Rho GTPases are known regulators of cytoskeletal dynamics and cell motility, and in fact RhoB is required for the NCC EMT (Liu and Jessell, 1998). Moreover, RhoGTPases are known to regulate multiple steps in the G1/S transition including Cyclin D1 protein accumulation (Tatsuno et al., 2000; Welsh et al., 2001). We found that *p27kip1* was upregulated by Sema3d knockdown, and there is considerable evidence that RhoGTPases are modulated by semaphorin signaling (Liu and Strittmatter, 2001; Pasterkamp and Kolodkin, 2003; Negishi et al., 2005). However, a specific role for Sema3d in modulating Rho GTPases remains to be tested.

Finally, our data do not rule out the possibility that Sema3d could regulate NCC migration independently of its effects on cell cycle. Semaphorins are well known for their role in directing migration of various cell types and may also regulate EMT and cell scattering. For example, semaphorins are upregulated in metastatic versus non-metastatic carcinoma cells (Christensen et al., 1998; Martin-Satue and Blanco, 1999; Brambilla et al., 2000). In addition, the plexin family of semaphorin receptors has significant homology to Met, the proto-oncogene and receptor for hepatocyte growth factor/scatter factor (Trusolino and Comoglio, 2002). Hepatocyte growth factor (HGF) can promote autocrine/paracrine-mediated cell dispersal (Stoker et al., 1987; Stella and Comoglio, 1999). Moreover, plexins can directly interact with Met (Giordano et al., 2002), suggesting crosstalk between these signaling pathways.

We thank Jeff Hardin, Anna Huttenlocher and members of the Halloran laboratory for critical reviews of this manuscript. We also thank R. Dorsky for the Tg(*hsp70*:ΔTCF^{gfp}) transgenic fish, and P. Henion, V. Prince and D. Raible for cDNAs. We thank the Zebrafish Information Resource Center for providing cDNAs and fish lines. This research was supported by NINDS grant NS42228 (M.C.H.) and NIGMS NRSA T32 GM07507 (J.D.B.). The NSF supported acquisition of the confocal microscope (NSF 9724515 to James Pawley, Department of Zoology, University of Wisconsin).

Supplementary material

Supplementary material for this article is available at http://dev.biologists.org/cgi/content/full/133/20/3983/DC1

References

Akimenko, M. A., Ekker, M., Wegner, J., Lin, W. and Westerfield, M. (1994). Combinatorial expression of three zebrafish genes related to distal-less: part of a homeobox gene code for the head. *J. Neurosci.* **14**, 3475-3486.

Aplin, A. E., Howe, A. K. and Juliano, R. L. (1999). Cell adhesion molecules, signal transduction and cell growth. *Curr. Opin. Cell Biol.* **11**, 737-744.

Bagnard, D., Vaillant, C., Khuth, S. T., Dufay, N., Lohrum, M., Puschel, A. W., Belin, M. F., Bolz, J. and Thomasset, N. (2001). Semaphorin 3A-vascular endothelial growth factor-165 balance mediates migration and apoptosis of neural progenitor cells by the recruitment of shared receptor. *J. Neurosci.* **21**, 3332-3341.

Barberis, D., Artigiani, S., Casazza, A., Corso, S., Giordano, S., Love, C. A., Jones, E. Y., Comoglio, P. M. and Tamagnone, L. (2004). Plexin signaling hampers integrin-based adhesion, leading to Rho-kinase independent cell rounding, and inhibiting lamellipodia extension and cell motility. *FASEB J.* **18**, 592-594.

Besson, A., Assoian, R. K. and Roberts, J. M. (2004). Regulation of the cytoskeleton: an oncogenic function for CDK inhibitors? *Nat. Rev. Cancer* **4**, 948-955.

Brambilla, E., Constantin, B., Drabkin, H. and Roche, J. (2000). Semaphorin SEMA3F localization in malignant human lung and cell lines: a suggested role in cell adhesion and cell migration. *Am. J. Pathol.* **156**, 939-950.

Bron, R., Eickholt, B. J., Vermeren, M., Fragale, N. and Cohen, J. (2004). Functional knockdown of neuropilin-1 in the developing chick nervous system by siRNA hairpins phenocopies genetic ablation in the mouse. *Dev. Dyn.* **230**, 299-308.

Brown, C. B., Feiner, L., Lu, M. M., Li, J., Ma, X., Webber, A. L., Jia, L., Raper, J. A. and Epstein, J. A. (2001). PlexinA2 and semaphorin signaling during cardiac neural crest development. *Development* **128**, 3071-3080.

Burstyn-Cohen, T. and Kalcheim, C. (2002). Association between the cell cycle and neural crest delamination through specific regulation of G1/S transition. *Dev. Cell* **3**, 383-395.

Burstyn-Cohen, T., Stanleigh, J., Sela-Donenfeld, D. and Kalcheim, C. (2004). Canonical Wnt activity regulates trunk neural crest delamination linking BMP/noggin signaling with G1/S transition. *Development* **131**, 5327-5339.

Chang, C. and Hemmati-Brivanlou, A. (1998). Neural crest induction by Xwnt7B in Xenopus. *Dev. Biol.* **194**, 129-134.

Chiang, E. F., Pai, C. I., Wyatt, M., Yan, Y. L., Postlethwait, J. and Chung, B. (2001). Two sox9 genes on duplicated zebrafish chromosomes: expression of similar transcription activators in distinct sites. *Dev. Biol.* **231**, 149-163.

Christensen, C. R., Klingelhofer, J., Tarabykina, S., Hulgaard, E. F., Kramerov, D. and Lukanidin, E. (1998). Transcription of a novel mouse semaphorin gene, M-semaH, correlates with the metastatic ability of mouse tumor cell lines. *Cell* **92**, 735-745.

D'Amico, M., Hulit, J., Amanatullah, D. F., Zafonte, B. T., Albanese, C., Bouzahzah, B., Fu, M., Augenlicht, L. H., Donehower, L. A., Takemaru, K. et al. (2000). The integrin-linked kinase regulates the cyclin D1 gene through glycogen synthase kinase 3beta and cAMP-responsive element-binding protein-dependent pathways. *J. Biol. Chem.* **275**, 32649-32657.

Danen, E. H. and Yamada, K. M. (2001). Fibronectin, integrins, and growth control. *J. Cell. Physiol.* **189**, 1-13.

De Wit, J., De Winter, F., Klooster, J. and Verhaagen, J. (2005). Semaphorin 3A displays a punctate distribution on the surface of neuronal cells and interacts with proteoglycans in the extracellular matrix. *Mol. Cell. Neurosci.* **29**, 40-55.

Duband, J. L., Monier, F., Delannet, M. and Newgreen, D. (1995). Epithelium-mesenchyme transition during neural crest development. *Acta Anat. Basel* **154**, 63-78.

Dutton, K. A., Pauliny, A., Lopes, S. S., Elworthy, S., Carney, T. J., Rauch, J., Geisler, R., Haffter, P. and Kelsh, R. N. (2001). Zebrafish colourless encodes sox10 and specifies non-ectomesenchymal neural crest fates. *Development* **128**, 4113-4125.

Eickholt, B. J., Mackenzie, S. L., Graham, A., Walsh, F. S. and Doherty, P. (1999). Evidence for collapsin-1 functioning in the control of neural crest migration in both trunk and hindbrain regions. *Curr. Biol.* **9**, R201-R204.

Feiner, L., Webber, A. L., Brown, C. B., Lu, M. M., Jia, L., Feinstein, P., Mombaerts, P., Epstein, J. A. and Raper, J. A. (2001). Targeted disruption of semaphorin 3C leads to persistent truncus arteriosus and aortic arch interruption. *Development* **128**, 3061-3070.

Ferrara, N., Gerber, H. P. and LeCouter, J. (2003). The biology of VEGF and its receptors. *Nat. Med.* **9**, 669-676.

Giordano, S., Corso, S., Conrotto, P., Artigiani, S., Gilestro, G., Barberis, D., Tamagnone, L. and Comoglio, P. M. (2002). The semaphorin 4D receptor controls invasive growth by coupling with Met. *Nat. Cell Biol.* **4**, 720-724.

Halloran, M. C., Severance, S. M., Yee, C. S., Gemza, D. L., Raper, J. A. and Kuwada, J. Y. (1999). Analysis of a Zebrafish semaphorin reveals potential functions in vivo. *Dev. Dyn.* **214**, 13-25.

Hay, E. D. (1995). An overview of epithelio-mesenchymal transformation. *Acta Anat. Basel* **154**, 8-20.

Hjorth, J. T. and Key, B. (2001). Are pioneer axons guided by regulatory gene expression domains in the zebrafish forebrain? High-resolution analysis of the patterning of the zebrafish brain during axon tract formation. *Dev. Biol.* **229**, 271-286.

Ito, Y., Oinuma, I., Katoh, H., Kaibuchi, K. and Negishi, M. (2006). Sema4D/plexin-B1 activates GSK-3beta through R-Ras GAP activity, inducing growth cone collapse. *EMBO Rep.* **7**, 704-709.

Jowett, T. (1999). Analysis of protein and gene expression. *Methods Cell Biol.* **59**, 63-85.

Kalcheim, C. and Burstyn-Cohen, T. (2005). Early stages of neural crest ontogeny: formation and regulation of cell delamination. *Int. J. Dev. Biol.* **49**, 105-116.

Kawasaki, T., Bekku, Y., Suto, F., Kitsukawa, T., Taniguchi, M., Nagatsu, I., Nagatsu, T., Itoh, K., Yagi, T. and Fujisawa, H. (2002). Requirement of neuropilin 1-mediated Sema3A signals in patterning of the sympathetic nervous system. *Development* **129**, 671-680.

Kelsh, R. N., Dutton, K., Medlin, J. and Eisen, J. S. (2000). Expression of zebrafish fkd6 in neural crest-derived glia. *Mech. Dev.* **93**, 161-164.

Kimmel, C. B., Warga, R. M. and Kane, D. A. (1994). Cell cycles and clonal strings during formation of the zebrafish central nervous system. *Development* **120**, 265-276.

Kimmel, C. B., Ballard, W. W., Kimmel, S. R., Ullmann, B. and Schilling, T. F. (1995). Stages of embryonic development of the zebrafish. *Dev. Dyn.* **203**, 253-310.

Kolodkin, A. L. (1998). Semaphorin-mediated neuronal growth cone guidance. *Prog. Brain Res.* **117**, 115-132.

LaBonne, C. and Bronner-Fraser, M. (1998). Neural crest induction in Xenopus: evidence for a two-signal model. *Development* **125**, 2403-2414.

Le Douarin, N. and Kalcheim, C. (1999). *The Neural Crest*. New York: Cambridge University Press.

Lewis, J. L., Bonner, J., Modrell, M., Ragland, J. W., Moon, R. T., Dorsky, R. I. and Raible, D. W. (2004). Reiterated Wnt signaling during zebrafish neural crest development. *Development* **131**, 1299-1308.

Liu, B. P. and Strittmatter, S. M. (2001). Semaphorin-mediated axonal guidance via Rho-related G proteins. *Curr. Opin. Cell Biol.* **13**, 619-626.

Liu, J. P. and Jessell, T. M. (1998). A role for rhoB in the delamination of neural crest cells from the dorsal neural tube. *Development* **125**, 5055-5067.

Liu, Y., Berndt, J., Su, F., Tawarayama, H., Shoji, W., Kuwada, J. Y. and Halloran, M. C. (2004). Semaphorin3D guides retinal axons along the dorsoventral axis of the tectum. *J. Neurosci.* **24**, 310-318.

Lumsden, A., Sprawson, N. and Graham, A. (1991). Segmental origin and migration of neural crest cells in the hindbrain region of the chick embryo. *Development* **113**, 1281-1291.

Luo, R., An, M., Arduini, B. L. and Henion, P. D. (2001). Specific pan-neural crest expression of zebrafish Crestin throughout embryonic development. *Dev. Dyn.* **220**, 169-174.

Martin-Satue, M. and Blanco, J. (1999). Identification of semaphorin E gene expression in metastatic human lung adenocarcinoma cells by mRNA differential display. *J. Surg. Oncol.* **72**, 18-23.

Miao, H. Q., Soker, S., Feiner, L., Alonso, J. L., Raper, J. A. and Klagsbrun, M. (1999). Neuropilin-1 mediates collapsin-1/semaphorin III inhibition of endothelial cell motility: functional competition of collapsin-1 and vascular endothelial growth factor-165. *J. Cell Biol.* **146**, 233-242.

Nasevicius, A. and Ekker, S. C. (2000). Effective targeted gene 'knockdown' in zebrafish. *Nat. Genet.* **26**, 216-220.

Negishi, M., Oinuma, I. and Katoh, H. (2005). Plexins: axon guidance and signal transduction. *Cell Mol. Life Sci.* **62**, 1363-1371.

Odenthal, J. and Nusslein-Volhard, C. (1998). fork head domain genes in zebrafish. *Dev. Genes Evol.* **208**, 245-258.

Osborne, N. J., Begbie, J., Chilton, J. K., Schmidt, H. and Eickholt, B. J. (2005). Semaphorin/neuropilin signaling influences the positioning of migratory neural crest cells within the hindbrain region of the chick. *Dev. Dyn.* **232**, 939-949.

Oxtoby, E. and Jowett, T. (1993). Cloning of the zebrafish krox-20 gene (krx-20) and its expression during hindbrain development. *Nucleic Acids Res.* **21**, 1087-1095.

Pasterkamp, R. J. and Kolodkin, A. L. (2003). Semaphorin junction: making tracks toward neural connectivity. *Curr. Opin. Neurobiol.* **13**, 79-89.

Perris, R. and Perissinotto, D. (2000). Role of the extracellular matrix during neural crest cell migration. *Mech. Dev.* **95**, 3-21.
Prince, V. E., Moens, C. B., Kimmel, C. B. and Ho, R. K. (1998). Zebrafish hox genes: expression in the hindbrain region of wild-type and mutants of the segmentation gene, valentino. *Development* **125**, 393-406.
Rubinstein, A. L., Lee, D., Luo, R., Henion, P. D. and Halpern, M. E. (2000). Genes dependent on zebrafish cyclops function identified by AFLP differential gene expression screen. *Genesis* **26**, 86-97.
Sakai, J. A. and Halloran, M. C. (2006). Semaphorin 3d guides laterality of retinal ganglion cell projections in zebrafish. *Development* **133**, 1035-1044.
Schilling, T. F. and Kimmel, C. B. (1994). Segment and cell type lineage restrictions during pharyngeal arch development in the zebrafish embryo. *Development* **120**, 483-494.
Schilling, T. F., Piotrowski, T., Grandel, H., Brand, M., Heisenberg, C. P., Jiang, Y. J., Beuchle, D., Hammerschmidt, M., Kane, D. A., Mullins, M. C. et al. (1996). Jaw and branchial arch mutants in zebrafish I: branchial arches. *Development* **123**, 329-344.
Serini, G., Valdembri, D., Zanivan, S., Morterra, G., Burkhardt, C., Caccavari, F., Zammataro, L., Primo, L., Tamagnone, L., Logan, M. et al. (2003). Class 3 semaphorins control vascular morphogenesis by inhibiting integrin function. *Nature* **424**, 391-397.
Shepard, J. L., Stern, H. M., Pfaff, K. L. and Amatruda, J. F. (2004). Analysis of the cell cycle in zebrafish embryos. *Methods Cell Biol.* **76**, 109-125.
Stella, M. C. and Comoglio, P. M. (1999). HGF: a multifunctional growth factor controlling cell scattering. *Int. J. Biochem. Cell Biol.* **31**, 1357-1362.
Stoker, M., Gherardi, E., Perryman, M. and Gray, J. (1987). Scatter factor is a fibroblast-derived modulator of epithelial cell mobility. *Nature* **327**, 239-242.
Sugrue, S. P. and Hay, E. D. (1981). Response of basal epithelial cell surface and Cytoskeleton to solubilized extracellular matrix molecules. *J. Cell Biol.* **91**, 45-54.
Tamagnone, L. and Comoglio, P. M. (2000). Signalling by semaphorin receptors: cell guidance and beyond. *Trends Cell. Biol.* **10**, 377-383.
Tamagnone, L. and Comoglio, P. M. (2004). To move or not to move? Semaphorin signalling in cell migration. *EMBO Rep.* **5**, 356-361.
Tammela, T., Enholm, B., Alitalo, K. and Paavonen, K. (2005). The biology of vascular endothelial growth factors. *Cardiovasc. Res.* **65**, 550-563.
Tan, C., Costello, P., Sanghera, J., Dominguez, D., Baulida, J., de Herreros, A. G. and Dedhar, S. (2001). Inhibition of integrin linked kinase (ILK) suppresses beta-catenin-Lef/Tcf-dependent transcription and expression of the E-cadherin repressor, snail, in APC–/– human colon carcinoma cells. *Oncogene* **20**, 133-140.
Tatsuno, I., Hirai, A. and Saito, Y. (2000). Cell-anchorage, cell cytoskeleton, and Rho-GTPase family in regulation of cell cycle progression. *Prog. Cell Cycle Res.* **4**, 19-25.
Tetsu, O. and McCormick, F. (1999). Beta-catenin regulates expression of cyclin D1 in colon carcinoma cells. *Nature* **398**, 422-426.
Thisse, C., Thisse, B. and Postlethwait, J. H. (1995). Expression of snail2, a second member of the zebrafish snail family, in cephalic mesendoderm and presumptive neural crest of wild-type and spadetail mutant embryos. *Dev. Biol.* **172**, 86-99.
Toyofuku, T., Yoshida, J., Sugimoto, T., Zhang, H., Kumanogoh, A., Hori, M. and Kikutani, H. (2005). FARP2 triggers signals for Sema3A-mediated axonal repulsion. *Nat. Neurosci.* **8**, 1712-1719.
Trusolino, L. and Comoglio, P. M. (2002). Scatter-factor and semaphorin receptors: cell signalling for invasive growth. *Nat. Rev. Cancer* **2**, 289-300.
Welsh, C. F., Roovers, K., Villanueva, J., Liu, Y., Schwartz, M. A. and Assoian, R. K. (2001). Timing of cyclin D1 expression within G1 phase is controlled by Rho. *Nat. Cell Biol.* **3**, 950-957.
Wolman, M. A., Liu, Y., Tawarayama, H., Shoji, W. and Halloran, M. C. (2004). Repulsion and attraction of axons by semaphorin3D are mediated by different neuropilins in vivo. *J. Neurosci.* **24**, 8428-8435.
Yu, H. H. and Kolodkin, A. L. (1999). Semaphorin signaling: a little less perplexin. *Mol. Cell Neurosci.* **13**, 9-23.
Yu, H. H. and Moens, C. B. (2005). Semaphorin signaling guides cranial neural crest cell migration in zebrafish. *Dev. Biol.* **280**, 373-385.
Yu, H. H., Houart, C. and Moens, C. B. (2004). Cloning and embryonic expression of zebrafish neuropilin genes. *Gene Expr. Patterns* **4**, 371-378.